THE JOURNAL OF PHYSICAL CHEMISTRY C LETTERS

2009, *113,* 16561–16564
Published on Web 08/31/2009

Nature of Oxidation of the Au(111) Surface: Experimental and Theoretical Investigation

Thomas A. Baker,[†] Bingjun Xu,[†] Xiaoying Liu,[†] Efthimios Kaxiras,*[,†,‡,§] and Cynthia M. Friend[†,‡]

Department of Chemistry and Chemical Biology, Harvard University, 12 Oxford Street, Cambridge, Massachusetts 02138, School of Engineering and Applied Sciences, Harvard University, Cambridge, Massachusetts 02138, and Department of Physics, Harvard University, 16 Oxford Street, Cambridge, Massachusetts 02139

Received: June 3, 2009

The Au(111) surface is the prototypical inert metal substrate, whose interaction with oxygen remains a controversial issue. Here, we study the effect of dosing temperature and coverage on the absorption of atomic oxygen on this surface, using *ab initio* molecular dynamics and high-resolution electron energy loss spectroscopy. Two vibrational peaks are observed experimentally at 380 and 580 cm^{-1}. The lower frequency peak is predominant at low oxygen coverages, while the higher frequency peak grows more pronounced with increasing oxygen coverage. Our simulations reproduce these results and show that oxygen chemisorbed on the surface is the primary species at low coverages or low surface temperatures. An oxide-like species, both on the surface and under the top layer of gold, becomes dominant at higher coverages or temperatures. These results elucidate the nature of oxidation of the Au(111) surface.

The Au(111) surface has long been considered the prototypical inert metal substrate, and a detailed understanding of the interaction of oxygen with this surface has become an important issue because oxidized Au(111) is a model for understanding chemical processes relevant to heterogeneous catalysis. The potential use of Au as a material for low-temperature selective oxidation catalysis has received renewed interest since the discovery of Haruta and others that gold nanoparticles supported on reducible metal oxides are active for such processes.[1−7] The adsorption of oxygen on gold is a complex process that has been studied both experimentally[8−12] and theoretically,[13−16] but leading to contradictory conclusions concerning the nature and structure of the adsorbed oxygen. Several different species of atomic oxygen on the surface have been proposed and observed including chemisorbed oxygen[10] and various forms of gold oxide.[9,11,12]

From the point of view of understanding the catalytic activity of gold, it is crucial to determine which oxygen species and structure prevail under different conditions. This can contribute toward improving and designing gold catalysts. Min et al.[17] found that the dosing temperature of atomic oxygen with ozone on Au(111) has a significant effect on the surface reactivity and selectivity to oxidation. Scanning tunneling microscopy (STM) studies revealed differences in the surface morphology depending on the temperature used for oxidation and the final coverage of oxygen; on the basis of this, it was proposed that different types of oxygen species (chemisorbed versus surface oxide) are responsible for the differences in reactivity.[17] The structure of the surface also plays a vital role, since the size[18,19] and particle shape[20] of oxide-supported Au nanoparticles have a substantial effect on the reactivity, with rate constants differing by as much as 2 orders of magnitude.[21] Also important but controversial is the potential role of subsurface oxygen in the chemistry of coinage metals.[22]

It is clear that temperature plays an important role in determining the morphology and ultimately the reactivity of the surface, but most of the theoretical work so far has employed static, zero temperature calculations based on density functional theory. This approach cannot capture the effect of temperature and does not allow for a thorough test of all the possible configurations of oxygen, as it relies only on structures determined *a priori*. Kinetic Monte Carlo (kMC) is a popular theoretical technique to model the dynamical and temperature dependent morphology of a surface,[23] although events important to the dynamics of the system need to be known before performing the simulation. Moreover, in kMC, the spatial degrees of freedom of the system are typically reduced to a lattice. Ideally, what is needed to capture all relevant effects is a fully atomistic molecular dynamics simulation with accurate forces between nuclei and with realistic conditions (temperature and oxygen concentration).

Toward this goal, we perform *ab initio* molecular dynamics simulations (AIMD) in the canonical ensemble,[24] with a time step of 3 fs, for the adsorption of oxygen on Au(111) in the framework of density functional theory using the VASP code[25] with the GGA-PW91[26] functional and ultrasoft pseudopotenitals.[27−29] The surface is modeled by a slab consisting of four layers in the (111) direction, with a 3×3 primitive unit cell in the lateral directions; the three uppermost layers of the slab were allowed to relax, with the bottom layer fixed at the ideal bulk positions. We consider different temperatures and coverages of

* Corresponding author. Address: Lyman Laboratory, 17 Oxford Street, Cambridge, MA, 02138. Phone: 617-495-7977. Fax: 617-496-2545. E-mail: kaxiras@physics.harvard.edu.
[†] Department of Chemistry and Chemical Biology.
[‡] School of Engineering and Applied Sciences.
[§] Department of Physics.

10.1021/jp9052192 CCC: $40.75 © 2009 American Chemical Society

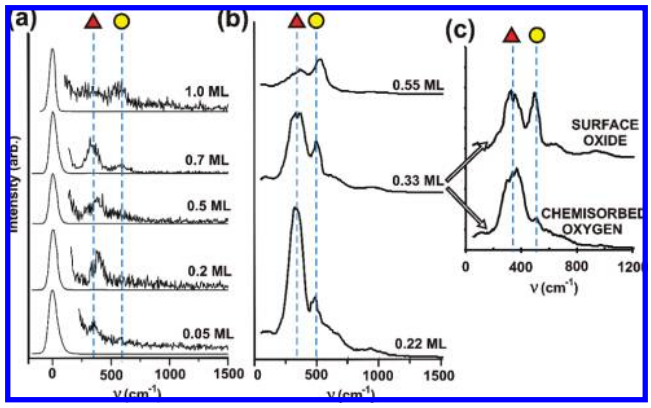

Figure 1. (a) HREEL spectra for increasing coverages of atomic oxygen dosed on Au(111) at 200 K. All spectra have been multiplied by a factor of 100. The two main peaks are identified with dotted lines at 380 and 580 cm^{-1} and labeled with a (red) triangle and (yellow) circle, respectively. (b) Calculated vibrational spectra for different coverages of atomic oxygen dosed at 500 K. The lower vibrational peak labeled by a (red) triangle is at 350 cm^{-1}, and the second peak labeled by a (yellow) circle is at 500 cm^{-1}. (c) Spectra from 0.33 ML oxygen coverage shown in cases corresponding to simulations that produced chemisorbed oxygen and surface oxide.

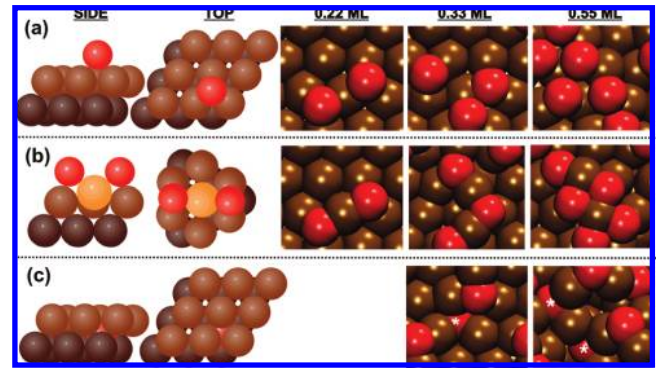

Figure 2. Model (left) and examples (right) of the three oxygen species: (a) chemisorbed; (b) surface oxide; (c) subsurface oxide. A prototypical model of each oxygen type is shown on the left. Dark brown, light brown, yellow, and red spheres represent the second layer of gold, top layer of gold, gold adatoms, and oxygen atoms, respectively. Illustrative examples of each oxygen type at each coverage are shown on the right. Brown and red spheres represent gold and oxygen atoms, respectively. An asterisk labels subsurface oxygen atoms in part c. We did not observe the subsurface oxide below an oxygen coverage of 0.33 ML.

oxygen and obtain the vibrational spectra through the velocity autocorrelation function. The calculated spectra are compared to experimental vibrational spectra obtained with high-resolution electron energy loss (HREEL).[30] We define the saturation coverage of atomic oxygen as 1.0 monolayer (ML), determined from quantitative temperature programmed desorption (TPD) experiments.

Two main vibrational features are identified experimentally at 380 and 580 cm^{-1} (Figure 1a) for atomic oxygen deposited by ozone decomposition on Au(111) at a surface temperature of 200 K. At lower coverages, only the lower vibrational peak at 380 cm^{-1} is present; the second peak at ~580 cm^{-1} grows as the coverage is increased, starting at ~0.5 ML of oxygen. The second peak dominates near saturation coverage. Recall that the surface is rough on the nanoscale, accounting for the relatively low signal:noise ratio and breadth of the peaks.

We simulated the adsorption of atomic oxygen on Au(111) at three different coverages (0.22, 0.33, and 0.55 ML) and at three different dosing temperatures (200, 500, and 800 K) and calculated the vibrational spectra, Figure 1b. Vibrational spectra are calculated from 20 independent trajectories by first equilibrating each system at the dosing temperature for 6 ps, then cooling to 200 K, and then running for an additional 6 ps. After changing the temperature to 200 K, 1.5 ps is elapsed to allow the system to reach equilibrium,[31] and the velocity autocorrelation function is calculated for the last 4.5 ps of the run. The gold substrate is equilibrated prior to oxygen adsorption for 1 ps starting from random velocities with kinetic energies corresponding to the dosing temperature. Atomic oxygen is then randomly placed, with random velocities corresponding to the dosing temperature, ~3 Å above the equilibrated Au(111) substrate.

The calculated vibrational spectrum and its dependence on oxygen coverage are nearly identical to the experimental results. At 500 K, Figure 1b, we observe two vibrational peaks at slightly lower frequencies than experiment, ~350 and ~500 cm^{-1}, with the higher frequency peak increasing in intensity with increasing oxygen coverage. There is a slight shift to higher frequencies for both peaks as the coverage increases; we attribute this shift to the increased oxygen−oxygen interactions due to the higher density of oxygen. For 0.22 ML of oxygen, the lower frequency peak could shift upward by as much as ~50 cm^{-1} for oxygen atoms adsorbed in adjacent 3-fold sites compared to the case when they are as far away as possible (~5 Å). While the shift to higher frequencies at higher oxygen coverage has been observed for similar systems, for example, O/Ru(0001),[32] the cause of this shift is not exactly clear.

We observe and subsequently categorize oxygen into three major species on the surface: (1) chemisorbed oxygen, (2) a 2D surface oxide, and (3) subsurface oxide.[33] Chemisorbed oxygen is characterized as oxygen bound on the top layer of the gold surface and coordinated to three surface gold atoms, shown in Figure 2a. The surface oxide contains groups of AuO_2 units where oxygen is bound on opposite sides of a gold atom that is pulled slightly out of the surface, shown in Figure 2b. These units can form chains of alternating oxygen and gold atoms generally growing in either straight or perpendicular directions similar to the structure found by Shi et al.[15] who determined this configuration to be the most favorable using static equilibrium density functional theory (DFT) thermodynamics calculations. Lastly, the subsurface oxide is characterized by oxygen diffusing anywhere below the top layer of gold atoms, as shown in Figure 2c.

To determine the contribution of each species to the total vibrational spectrum, we average and group together molecular dynamics runs that produce the same oxygen species. For example, Figure 1c shows the vibrational results for 0.33 ML oxygen dosed at 500 K but split into simulations that result in the chemisorbed oxygen and simulations that produce some surface oxide. A vibrational peak at ~350 cm^{-1} is present in the simulated spectra for both types of species, but the peak at ~500 cm^{-1} is missing in the spectrum for chemisorbed oxygen. This vibrational pattern is the same for different oxygen coverages and dosing temperatures; namely, the second higher-frequency peak is not present for chemisorbed oxygen but is present for the surface oxide. There are no significant differences in the simulated spectra of the surface oxide and the subsurface oxide, suggesting that the higher frequency peak is due to either the surface oxide or the subsurface oxide and not to chemisorbed oxygen.

In both the experimental and computational results, as the oxygen coverage increases, so does the second vibrational peak.

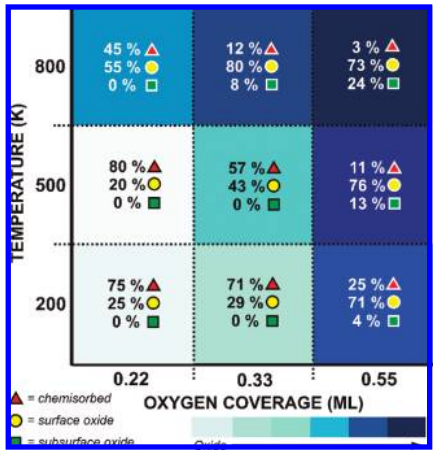

Figure 3. Diagram illustrating the percentage of each oxygen type at each dosing temperature and oxygen coverage. Each square is shaded by the amount of oxide character of the surface, calculated by considering the chemisorbed oxygen as the least "oxide-like" and the subsurface oxide as the most "oxide-like".

On the basis of these results, we conclude that chemisorbed oxygen dominates at low coverages of oxygen, while the oxide is observed at higher coverages. Figure 3 confirms this conclusion by illustrating the percentage of each oxygen species on the surface at different coverages or dosing temperatures. For example, at a low oxygen coverage and dosing temperature (0.22 ML and 200 K), there is a large percentage of chemisorbed oxygen (75%), a smaller percentage of surface oxide (25%), and no subsurface oxide. At a high oxygen coverage and dosing temperature (0.55 ML and 800 K), there is a much larger percentage of surface oxide (73%) and subsurface oxide (24%) and very little chemisorbed oxygen (3%), confirming our conclusion. In previous static DFT calculations, we found that a chemisorbed oxygen vibration is normal to the surface at a frequency similar to this work.[34] Our results also agree well with previous work based on static DFT calculations, where we found that gold incorporation becomes more favorable at higher coverages of Cl or O.[35] In that case, as the coverage increases, the bonding between the adsorbate and gold becomes more covalent in nature, reducing the partial charge on the oxygen which allows oxygen atoms to pack closer together. Presumably the same is true in the present case and could explain the roughening of the surface at higher coverages.

Our results also agree well with previous experimental studies. At each coverage and temperature we considered, there is at least some small amount of surface oxide, see Figure 3, consistent with STM observations where there was always some release of gold atoms to form islands on the surface even at low coverages of oxygen.[17] This is especially true for adsorption of oxygen on the "herringbone" reconstruction of Au(111) which contains an extra 4.5% gold atoms in the top layer that can easily be removed by interaction with adsorbates.[36,37] Our work also supports the previous suggestion that the 2D and 3D islands observed by STM at higher dosing temperatures and coverages are a gold oxide, since our calculation, Figure 3, suggests that at higher temperatures the surface should be more oxidic in character.[38]

Previous work demonstrated that at lower coverages of oxygen dosed at 200 K, which corresponds to just the presence of the lower vibrational peak in HREELS, Au(111) was the most reactive and selective for oxidation of carbon monoxide as well as other hydrocarbons, and that the surface becomes less reactive at higher dosing temperatures or coverages.[16] We have identified the lower frequency peak in vibrational spectroscopy as corresponding to chemisorbed oxygen from our AIMD simulations and that this species is dominant at lower coverages and dosing temperatures. This also agrees with our previous work showing that oxygen binds stronger when incorporated with gold adatoms at higher coverages or when bound on steps or vacancies.[34] These conclusions, based on a systematic and unbiased theoretical investigation with AIMD simulations at various temperatures and oxygen coverages, provide fundamental insight into the reactivity of gold by identifying chemisorbed oxygen as the active species for oxidation on Au(111).

Finally, an important consequence of our calculations is the ability to understand the kinetic processes responsible for the formation of the surface and subsurface oxide. The energy barrier, estimated from variations in the total energy, for the formation of the surface oxide is smaller than 0.1 eV, that for the formation of subsurface oxide is in the range 0.8−1.4 eV, and the barrier for chemisorbed oxygen diffusion is in the range 0.2−0.6 eV. The surface oxide forms when two oxygen atoms diffuse to 3-fold sites that share a gold atom in the surface between them, as shown in the 0.22 ML example in Figure 2a. This is the dominant but not the sole mechanism, especially at higher temperatures when the surface is very disordered. After this diffusion, it takes ~600−1000 fs for the gold atom attached to the two oxygen atoms to lift out of the surface and form the surface oxide, shown in the 0.22 ML example in Figure 2b. The process for formation of the subsurface oxide starts with one or several oxygen atoms lifting a surface gold atom, followed by an additional nearby oxygen atom diffusing to fill some of the vacancy left behind by the lifted gold atom. This often occurs when the surface oxide (AuO_2) is formed with a third oxygen atom nearby to form the subsurface oxide. A complete analysis of the kinetics for the formation of the gold oxide will be the subject of future work.

Acknowledgment. This work was funded in part by a graduate school fellowship from the National Science Foundation, a NSF grant via Harvard NSEC, Grant No. PHYS-0646094 U.S., and a grant from the Department of Energy, Basic Energy Sciences, under Grant No. FG02-84-ER13289. The authors would like to thank the High Performance Computing cluster at the Harvard School of Engineering and Applied Sciences.

References and Notes

(1) Haruta, M. *Chem. Rec.* **2003**, *3*, 75.
(2) Haruta, M.; Date, M. *Appl. Catal., A* **2001**, *222*, 427.
(3) Meyer, R.; Lemire, C.; Shaikhutdinov, S. K.; Freund, H. *Gold Bull.* **2004**, *37*, 72.
(4) Haruta, M.; Yamada, N.; Kobayashi, T.; Iijima, S. *J. Catal.* **1989**, *115*, 301.
(5) Hayashi, T.; Tanaka, K.; Haruta, M. *J. Catal.* **1998**, *178*, 566.
(6) Grisel, R. J. H.; Kooyman, P. J.; Nieuwenhuys, B. E. *J. Catal.* **2000**, *191*, 430.
(7) Jang, B. W. L.; Spivey, J. J.; Kung, M. C.; Kung, H. H. *Energy Fuels* **1997**, *11*, 299.
(8) Saliba, N.; Parker, D. H.; Koel, B. E. *Surf. Sci.* **1998**, *410*, 270.
(9) Chesters, M. A.; Somorjai, G. A. *Surf. Sci.* **1975**, *52*, 21.
(10) Canning, N. D. S.; Outka, D.; Madix, R. J. *Surf. Sci.* **1984**, *141*, 240.
(11) Pireaux, J. J.; Liehr, M.; Thiry, P. A.; Delrue, J. P.; Caudano, R. *Surf. Sci.* **1984**, *141*, 221.
(12) Parker, D. H.; Koel, B. E. *J. Vac. Sci. Technol., A* **1990**, *8*, 2585.
(13) Mavrikakis, M.; Stoltze, P.; Norskov, J. K. *Catal. Lett.* **2000**, *64*, 101.
(14) Liu, Z. P.; Hu, P.; Alavi, A. *J. Am. Chem. Soc.* **2002**, *124*, 14770.
(15) Shi, H.; Stampfl, C. *Phys. Rev. B* **2007**, *76*, 075327.
(16) Miller, S. D.; Kitchin, J. R. *Surf. Sci.* **2008**, *603*, 794.
(17) Min, B. K.; Alemozafar, A. R.; Pinnaduwage, D.; Deng, X.; Friend, C. M. *J. Phys. Chem. B* **2006**, *110*, 19833.

(18) Valden, M.; Lai, X.; Goodman, D. W. *Science* **1998**, *281*, 1647.
(19) Valden, M.; Pak, S.; Lai, X.; Goodman, D. W. *Catal. Lett.* **1998**, *56*, 7.
(20) Comotti, M.; Li, W. C.; Spliethoff, B.; Schuth, F. *J. Am. Chem. Soc.* **2006**, *128*, 917.
(21) Lopez, N.; Janssens, T. V. W.; Clausen, B. S.; Xu, Y.; Mavrikakis, M.; Bligaard, T.; Norskov, J. K. *J. Catal.* **2004**, *223*, 232.
(22) Qu, Z.; Cheng, M.; Huang, W.; Bao, X. *J. Catal.* **2005**, *229*, 446.
(23) Battaile, C. C.; Srolovitz, D. *Annu. Rev. Mater. Res.* **2002**, *32*, 297.
(24) Nose, S. *Mol. Phys.* **2002**, *100*, 191.
(25) Kresse, G.; Hafner, J. *Phys. Rev. B* **1993**, *47*, 558.
(26) Perdew, J. P.; Wang, Y. *Phys. Rev. B* **1992**, *45*, 13244.
(27) Kresse, G.; Hafner, J. *J. Phys.: Condens. Matter* **1994**, *6*, 8245.
(28) Vanderbilt, D. *Phys. Rev. B* **1990**, *41*, 7892.
(29) We used a plane-wave cutoff energy of 300.0 eV, an electronic convergence tolerance of 10^{-3} eV, and $2 \times 2 \times 1$ Monkhorst-Pack *k*-point sampling.
(30) HREELS experiments were performed in a stainless steel vacuum chamber with a base pressure of $\sim 2 \times 10^{-10}$ Torr. The oxygen covered Au(111) surface was prepared by ozone exposure, as described in detail elsewhere.[17] All spectra were collected at 200 K with a beam energy of 6.91 eV. The typical full width at half maximum of the elastic peak was ~ 70 cm^{-1}.
(31) It is known from temperature programmed desorption experiments that the desorption temperature of atomic oxygen from the surface of gold is ~550 K. Because of the time scales that are accessible in the calculations (6 ps), even at a dosing temperature of 800 K, desorption is not observed, since we do not reach true equilibrium. However, we do reach a pseudo-equilibrium (as evidenced by the nearly constant energy and other measurable quantities throughout the simulation) and the higher temperature allows us to model the morphological changes in the time scale accessible by our calculations.
(32) He, P.; Jacobi, K. *Phys. Rev. B.* **1997**, *55*, 4751.
(33) There is not a clear definition in the literature of "surface oxide" and "subsurface oxide". We only use these terms to classify the location of oxygens observed in our simulations. The structure we observe for the subsurface oxide is not the structure of the bulk gold oxide; however, the short time scales accessible in our simulations preclude us from ruling out an oxide structure. Additional work is planned to better understand the bonding and the charge distribution of these different oxygen states.
(34) Baker, T. A.; Friend, C. M.; Kaxiras, E. *J. Phys. Chem. C* **2009**, *113*, 3232.
(35) Baker, T. A.; Friend, C. M.; Kaxiras, E. *J. Chem. Phys.* **2009**, *130*, 084701.
(36) Narasimhan, S.; Vanderbilt, D. *Phys. Rev. Lett.* **1992**, *69*, 1564.
(37) Min, B. K.; Deng, X.; Pinnaduwage, D.; Schalek, R.; Friend, C. M. *Phys. Rev. B* **2005**, *72*, 4.
(38) Some of the 2D and 3D oxides formed experimentally are ordered. Because of the constraints on the unit cell size in our calculations, we cannot expect to determine the exact structure of these oxides; rather, we may be finding the precursors to their formation.

JP9052192